Published in final edited form as:
Eur J Neurosci. 2011 February ; 33(3): 433–443. doi:10.1111/j.1460-9568.2010.07537.x.

Cholinergic and non-cholinergic mesopontine tegmental neurons projecting to the subthalamic nucleus in the rat

Takako Kita and **Hitoshi Kita**
Department of Anatomy and Neurobiology, College of Medicine, University of Tennessee, Memphis, Tennessee 38163

Abstract

The subthalamic nucleus (STN) receives cholinergic and non-cholinergic projections from the mesopontine tegmentum. This study investigated the numbers and distributions of neurons involved in these projections in rats using Fluorogold (FG) retrograde tracing combined with immunostaining of choline acetyltransferase and a neuron-specific nuclear protein. The results suggest that a small population of cholinergic neurons mainly in the caudoventral part of the pedunculopontine tegmental nucleus (PPN), approximately 360 neurons (≈10% of total) in the homolateral and 80 neurons (≈2%) in the contralateral PPN, projects to the STN. In contrast, the number of non-cholinergic neurons projecting to the STN was estimated to be 9 times as much, with approximately 3300 in the homolateral side and 1300 neurons in the contralateral side. A large gathering of the FG-labeled non-cholinergic neurons was found rostrodorsomedial to the caudolateral PPN. The biotinylated dextran amine (BDA) anterograde tracing method was used to substantiate the mesopontine-STN projections. Injection of BDA into the caudoventral PPN labeled numerous thin fibers with small en-passant varicosities in the STN. Injection of BDA into the non-cholinergic neuron-rich area labeled a moderate number of thicker fibers with patches of aggregates of larger boutons. The densities of labeled fibers and the number of retrogradely labeled cells in the mesopontine tegmentum suggested that the terminal field formed in the STN by each cholinergic neuron is more extensive than that by each non-cholinergic neuron. The findings suggest that cholinergic and non-cholinergic mesopontine afferents may carry different information to the STN.

Keywords

pedunculopontine tegmentum; subthalamic nucleus; cholinergic projection

Introduction

The mesopontine tegmentum is a complex reticular structure that is involved in various sensorimotor, associative, sleep wakefulness, and limbic functions. The mesopontine tegmentum receives inputs from basal ganglia output nuclei. In turn, the mesopontine tegmentum projects back to several nuclei in the basal ganglia including the subthalamic nucleus (STN). These connections imply that one of the roles of the mesopontine tegmentum is to monitor the level of the basal ganglia outputs and to control the level of activity of the basal ganglia (Mena-Segovia et al., 2004). Pathological changes of the mesopontine tegmentum in patients with motor disorders have been known (Hirsch et al., 1987; Jellinger, 1988; Zweig et al., 1989). Recent studies report the effectiveness of lesions

Correspondence to: Hitoshi Kita, Department of Anatomy and Neurobiology, College of Medicine, The University of Tennessee Memphis, 855 Monroe Avenue, Memphis, TN 38163. Phone: 901-448-5234, Fax: 901-448-7193, hkita@uthsc.edu.

and deep brain stimulation of the PPN of Parkinson's disease (PD) patients and animal models of PD (Jenkinson et al., 2004; Plaha & Gill, 2005; Stefani et al., 2007, 2009). Considering the effectiveness of lesions and deep brain stimulation of STN, it is possible that the mesopontine-STN projections play a significant role in the development of abnormal activity of STN neurons in PD subjects and in the therapeutic effects of the lesions and stimulations of PPN. These possibilities may be addressed by experimental studies using rodents. However, because the extent and the location of neurons participating in the mesopontine-STN projections have not yet been fully characterized, it is difficult to conduct physiological and behavioral studies based on current knowledge.

The mesopontine tegmentum contains two cholinergic cell groups: Ch5 and Ch6 (Mesulam et al., 1983). The area containing Ch5 and Ch6 neurons are often referred to as the pedunculopontine tegmental nucleus (PPN) and the laterodorsal tegmental nucleus (LDT), respectively. Both the PPN and LDT contain numerous non-cholinergic, mostly glutamatergic and GABAergic, neurons in addition to the cholinergic neurons (Clements and Grant, 1990; Grofova & Zhou, 1998; Manaye et al., 1999; Wang & Morales, 2009; Mena-Segovia et al., 2009). The non-cholinergic mesopontine tegmentum includes several areas including the retrorubral field, the deep mesencephalic nucleus, and the oral part of the pontine reticular nucleus.

The aims of the present study were to gain insights on following issues: Several reports described the involvement of both cholinergic and non-cholinergic neurons in mesopontine-STN projections (Woolf & Butcher, 1986; Semba & Fibiger 1992; Bevan & Bolam, 1995: Mena-Segovia et al., 2004). However, others de-emphasize the involvement of the cholinergic projection and place more importance on the non-cholinergic projections (Jackson & Crossman, 1981; Rye et al., 1987, Hallanger & Wainer, 1988; Lee et al., 1988; Carpenter & Jayaraman, 1990; Steininger et al., 1992). Therefore, the first aim of the present study was to establish the existence of cholinergic mesopontine-STN projections and to investigate the locations and populations of the Ch5 and Ch6 neurons participating in the projections. The second aim was to study the location and population of non-cholinergic neurons participating in the projections. The third aim was to investigate the relative numbers of neurons involved in the contralateral over homolateral cholinergic and non-cholinergic mesopontine-STN projections.

Methods

Animal preparation and brain sectioning

All procedures were approved by the institutional animal care and use committee and conformed to NIH guidelines. A total of 33 male Sprague-Dawley rats (280–380 g, Charles River Laboratories, Wilmington, MA, USA) were used in this study. Four of the rats were used for immunohistochemical examinations of ChAT-immunoreactive (ChAT+) neurons in the mesopontine tegmentum and fibers in the STN. Two of the 4 rats received electric lesions in the left midbrain tegmentum to cut mesopontine-STN fibers. For the lesions, rats were anesthetized (i.p.) with a mixture of ketamine (60mg/kg, Pfizer, Inc. New York City, NY, USA) and xylazine (10mg/kg, Agri Lab. St. Joseph, MO, USA) and placed on a stereotaxic apparatus. A craniotomy over the SNc was made and a glass-insulated tungsten electrode was penetrated 1.2, 2.0, and 2.8 mm from the midline and all at 3.5 mm rostral to the interaural line. Two lesions per penetration, one at the level of the substantia nigra pars compacta (SNc) and another 0.7 mm dorsal to the first lesion, were made by passing a 400 μA cathode current for 10 sec through the electrode. These rats survived for 10 days.

The Fluorogold (FG, Fluorochrome, LLC. Denver, CO, USA) retrograde labeling method introduced by Schmued & Fallon (1986) was used to label the mesopontine-STN and

mesopontine-zona incerta (ZI) neurons. The FG method was used because of its superior sensitivity compared to cholera toxin B subunit and rhodamine-labeled microsphere methods. It was also difficult to cover a large portion of the STN with cholera toxin B subunit and rhodamine-labeled microspheres using our injection method without creating obvious tissue damage in STN. These pilot experiments indicated that FG was the most sensitive retrograde marker and therefore was the best suited to fulfill the aims of the present study to reveal all the possible origins of the mesopontine-STN projections. FG was injected into the STN of 12 rats, and control FG injections were made into the ZI of 7 rats. For the FG injections, glass micropipettes (tip diameter approximately 10 μm) glued to the needle of a 10μl Hamilton microsyringe were filled with 0.2–0.3% FG in saline. The rats were anesthetized, and craniotomy over the STN and ZI was made for the insertion of the pipette as described above. X-ray images (Model 275, Minxray Inc. Northbrook, IL, USA) of the rats' heads and the shank of the glass pipette aided the antero-posterior placement of the pipettes. Extracellular firing activity detected through the micropipette was amplified by a homemade amplifier and was fed to an oscilloscope and an audiomonitor to detect the activity of STN and ZI neurons. FG (0.1 μl) was injected slowly (0.02 μl/min) by pushing the microsyringe plunger with an electric actuator. The concentration and volume of FG necessary to produce an injection site comparable to the size of STN was determined after several trial experiments.

A biotinylated dextran amine (BDA) anterograde tracing method was used to label the mesopontine-STN axons and to confirm the results of retrograde tracing experiments. An advantage of the BDA method over others such as the *Phaseolus vulgaris-leucoagglutinin* method is that the visualization requires no immunohistochemical procedures. The BDA method used in this study differed from the method used to visualize the collateral axons of Golgi-like retrogradely labeled cells (Reiner et al., 2000). BDA (0.1 μl, 3% dissolved in 0.01 M phosphate buffer pH 7.2, BDA-10000, Molecular Probes, Eugene, OR, USA) was pressure-injected into the left mesopontine tegmentum in 10 rats using a method similar to the FG injection described above. The injection produced injection sites with a diameter of about 0.5 mm. The survival period of the rats injected with FG or BDA was 7–10 days.

All the rats were deeply anesthetized with a mixture of ketamine (100 mg/Kg) and xylazine (20 mg/Kg) and were perfused through the heart with 10 to 20 ml of isotonic saline followed by a fixative. The fixative was a mixture of 4% formaldehyde and 0.2% picric acid in a 0.12 M sodium phosphate buffer (200–300 ml, pH 7.4). After perfusion, the brains were removed and postfixed overnight at 4°C and then equilibrated in a 10% followed by a 30% sucrose in phosphate buffer (pH 7.4). All the chemicals used for making the fixative, buffers, and other histological solutions were obtained from Sigma-Aldrich (St. Louis, MO, USA). The brains for ChAT immunostaining were cut into 30 μm sagittal sections on a freezing microtome. The brains for FG and BDA tracings were cut into coronal sections since the use of coronal plains was the most common method in previous publications. The 30 μm serial sections were divided into 8 sets for single labeling with FG or BDA or for double or triple labeling with other markers as described below.

Immunohistochemistry for FG

All the sections used for immunohistochemistry were pre-incubated in phosphate buffered (pH 7.6) saline (PBS) containing 0.5% non-fat dry milk and 0.2% Triton-X for 2–3 hours and then incubated overnight in PBS containing rabbit anti-FG serum (1:15,000, a gift from Dr. H.T. Chang). The sections were rinsed 4 times with PBS and incubated in biotinylated anti-rabbit antibody (0.5 μg/ml, BA-1000, Vector Laboratories, Burlingame, CA, USA) for 1.5 hours. Next, the sections were rinsed 4 times with PBS and incubated in an avidin-biotin-peroxidase complex (ABC, 1:100, Vector Laboratories, Burlingame, CA, USA) for 1.5 hours. Finally, the sections were rinsed 4 more times and then incubated in PBS

containing 3,3′-diaminobenzidine (DAB, 0.05%, NiCl (0.001%), and H_2O_2 (0.003%). This reaction resulted in dark blue granular reaction products in the cytoplasm of FG-labeled (FG +) neurons with virtually no non-specific background staining. The specificity of the FG antiserum was tested by staining brain sections obtained from a rat without FG injection as well as by omission of the primary antiserum (Chang et al., 1990).

Visualization of BDA

For the visualization of BDA, sections were rinsed with PBS and then incubated in PBS containing 2 % ABC and 0.2% Triton X-100 for 3 hours. After rinsing several times with PBS, the sections were incubated in PBS containing 3,3′-diaminobenzidine (0.05%), NiCl (0.001%), and H_2O_2 (0.003%). This process stained the BDA-labeled axons dark-blue.

Multiple staining

Some of the sections stained for BDA and FG were further processed for immunostaining for ChAT or neuron-specific nuclear protein (NeuN). The goat anti-ChAT serum (Millipore, AB144, Billerica, MA, USA) recognizes a single band of 68–70 kD on Western blot of rat brains (information provided by Millipore). The NeuN monoclonal antibody (MAB377, Millipore) recognizes NeuN in most central nervous systems of vertebrates (information provided by Millipore). The sections were incubated overnight in PBS containing anti-ChAT (1:200) or anti-NeuN (1:2000), followed by biotinylated anti-goat antibody or biotinylated anti-mouse antibody (0.5 μg/ml, BA-5000 and BA-2000, Vector Laboratories, Burlingame, CA, USA) for 1.5 hour and ABC. The peroxidase was then visualized by incubating the sections in PBS containing 3,3′-diaminobenzidine (0.05%) and H_2O_2 (0.003%). The immunostaining for ChAT stained the cytoplasm of cholinergic neurons a yellow-brown color. The immunostaining for NeuN stained the nuclei neurons a yellow-brown color and stained the cytoplasm a light yellow color. Some of the FG and ChAT doubly stained sections were selected for third immunohistochemistry for NeuN. These selected sections were incubated overnight with the antibody for NeuN, followed by biotinylated anti-mouse antibodies and then by ABC. The peroxidase was then visualized by the Vector® VIP substrate kit following the instructions provided with the kit. This reaction stained the nuclei and cytoplasm of the neurons purple. After several rinses, immunostained sections were mounted on gelatin-coated slides, air-dried, dehydrated in graded alcohols to xylene, and coverslipped. For the analyses, a total of 8 sections from every 8 serial sections were chosen such that the first and the second of the 8 sections contained the 3^{rd} and 4^{th} nuclei, respectively. The locations of the first and last sections corresponded approximately to that of the interaural 2.16 mm and 0.48 mm plains of the rat brain atlas by Paxinos and Watson (1998), although the cut angle was slightly different from that in the atlas.

Somata of neurons with nucleus and stained with FG, ChAT, or NeuN in the retrorubral field (RRF), PPN, LDTv, the deep mesencephalic nucleus (DMN), and the pontine reticular nucleus oral part (PnO) were drawn using a light microscope with x40 objective and a camera lucida (Olympus BX50). The criterion for the double labeling of neurons for FG and ChAT or FG and NeuN was the existence of multiple dark blue granular FG reaction products in yellow-brown or yellow stained cytoplasm. The single versus double staining could be unquestionably determined in most of neurons. Questionable neurons were categorized by observation using an x100 oil-immersion objective. The numbers of FG+ and ChAT+ neurons were estimated by counting neurons in every 8^{th} of 30 μm serial sections. The use of 30 μm Triton-X treated frozen sections was to ensure good penetration of immunoreagents and also to reduce chances of overlapping neurons in the Z-axis. Neurons located at the surface of the sections were included or rejected for the cell count based on judgment that more than half of their nucleus remained in the section. The judgments were made by observing outline of each nucleus through change of focal plane and by comparing

the nucleus with nuclei of intact neurons of similar size located nearby. The diameter of the nucleus with more than half remaining in the section should be similar to the intact nuclei. The method may result in a slight overestimate by including neurons having slightly less than half of the nucleus. Some of the mesopontine nuclei including the PPN have no clear boundaries, and neurons in these nuclei are unevenly distributed. We considered counting the neurons in the defined thickness of sections obtained from entire rostrocaudal extension of the area of interest provide a reasonable estimate of the number of sparse population of neurons distributed in a wide area such as FG+/ChAT+ neurons. Somatic sizes of neurons were estimated from camera lucida drawings with an x100 oil-immersion objective of 200 neurons with no obvious cuts to the somata in each group. The size of the area in the outline of soma was measured using the NIH Image 6 software, and Student's *t*-test was used to evaluate the size differences. Microscopic images were acquired by a digital camera (Nikon D70) and processed using a Macintosh computer with Photoshop (Adobe) and Canvas (Deneva).

Results

ChAT-immunopositive afferent fibers

Immunohistochemistry for ChAT visualized cholinergic neurons and their fibers (Fig. 1). Sagittal and coronal sections revealed that the rostral and caudomedial parts of PPN contained sparse ChAT+ neurons and the caudolateral PPN contained dense ChAT+ neurons (e.g., Fig. 1A and Fig. 2), as reported previously (Mena-Segovia et al., 2009). The ventrally coursing ascending ChAT+ fibers from PPN travel mainly through the SNc and the dorsally adjacent area and innervate in the STN and ZI. The STN was more densely innervated by ChAT+ fibers than ZI (Fig. 1A). The fibers traverse through the STN from the caudodorsal to the rostroventral direction and emit thin branches with numerous small boutons en-passant (Fig. 1B). Some of the fibers exit STN in the rostroventral direction.

The electric lesion of the midbrain tegmentum extended from deep layers of the superior colliculus to SNc (Fig. 1C) with mediolateral extension of approximately 1–3 mm from the midline. The lesion greatly reduced ChAT+ fibers in the STN and ZI. However, some of the fibers that originated from the contralateral PPN and traveled medial to the lesion survived. A few fibers that originated from the ipsilateral PPN and traveled through the substantia nigra pars reticulata (SNr) also escaped the lesion.

FG injection into STN

The FG injections were aimed at the middle of the STN with the aid of x-ray imaging and unit recording. Of the 12 injections made, 4 covered most of the STN with very little spreading to the ZI (Fig. 2A), and the other 8 covered a portion of the STN with greater spreading to the ZI. Figure 2B shows a mesopontine section immunostained for FG, ChAT, and NeuN. Neurons labeled with FG and ChAT (FG+/ChAT+), ChAT+ but FG negative (FG−/ChAT+), FG+ and immunoreactive for NeuN (NeuN+, i.e., non-cholinergic, FG+/ChAT−), and FG negative NeuN+ (FG−/ChAT−) neurons are visible. FG+/ChAT+ neurons often contained a dense accumulation of FG-immunoreactive granules, so these neurons could be easily distinguished from FG−/ChAT+ neurons. This was not due to the masking of faint labeling by the staining for ChAT because the sections that were stained only for FG also showed strongly labeled large neurons and only rarely faintly labeled large ones (data not shown). On the other hand, the density of FG granules in non-cholinergic (ChAT−) neurons was variable (Fig. 2D).

Locations of mesopontine-STN projection neurons

The PPN in rats has often been subdivided into the pars dissipata, subpeduncular tegmental nucleus, and pars compacta. Although ChAT immunohistochemistry revealed the general areas containing dense or sparse ChAT+ neurons as described above, the borders between these subdivisions could not be clearly defined. Additionally, since all subdivisions contained non-cholinergic neurons (Grofova & Zhou, 1998; Manaye et al., 1999; Mena-Segovia et al., 2009; Wang & Morales, 2009), there was no visible difference in the total cell densities of the subdivisions of PPN. Because of this, the measurements of the somatic sizes and numbers of ChAT+ neurons in the PPN subdivisions were not separated in the present study. The LDTv could be identified as a nucleus dense with cholinergic and non-cholinergic neurons. Also, the dendritic arbor of cholinergic neurons often was confined to the nucleus. For the somatic size and cell count analysis of FG+/ChAT− neurons, the neurons in RRF, PPN, the ventral part of DMN, and in the very dorsal most part of PnO were grouped because of the difficulty in delineating the borders between these areas. The dorsal part of the DMN and the middle to ventral parts of PnO did not contain FG+ neurons.

Sizes of mesopontine-STN projection neurons

The somatic sizes of FG+/ChAT+ (370.6 ± 71.8 μm^2, mean±S.D., n=200) and FG−/ChAT+ PPN neurons (379.9 ± 74.6 μm^2, n=200) were similar (t=1.58, p=0.12). The sizes of FG+/ChAT− (197.4 ± 42.5 μm^2, n=200) and FG−/ChAT− neurons (217.7 ± 42.1 μm^2, n=200) in the mesopontine tegmentum were also similar (t=1.71, p=0.89). The ChAT+ neurons are almost two times larger than ChAT− neurons (t=28.4, p<0.0001). The sizes of ChAT+ and ChAT− neurons were very similar to those reported by a juxtacellular labeling study (Mena-Segovia et al., 2008). In the LDTv, the sample size of the FG+/ChAT+ neurons was too small to be compared statistically with FG−/ChAT− neurons. However, the sizes of FG−/ChAT+ (397.3 ± 45.8 μm^2, n=200) and FG−/ChAT− neurons (202.4 ± 49.1 μm^2, n=200) in the LDTv could be compared and were found to be significantly different (t=32.4, p<0.0001).

Numbers of ChAT+ mesopontine-STN projection neurons

The cell count analyses were performed on the 4 cases that had FG injection sites covering most of the STN with very little spreading to the ZI (Fig. 2A). Figure 3A shows the numbers of FG+/ChAT+, FG−/ChAT+, and FG+/ChAT− neurons observed in the mesopontine tegmentum of the 8 sections collected from every 8^{th} cut. The tables in Figure 3 show the total numbers of FG+/ChAT+ and FG−/ChAT+ neurons in the PPN and LDTv (Fig. 3B) and FG+/ChAT− neurons in the mesopontine tegmentum (Fig. 3C). There were 31–56 FG+/ChAT+ neurons in the PPN of the 8 sections ipsilateral to the FG-injected STN. These numbers represented 7.2–12.2% of total ChAT+ neurons in the PPN. The contralateral PPN contained approximately 20% of the total FG+/ChAT+ neurons found in the ipsilateral PPN. Though the LDTv contained fewer FG+/ChAT+ neurons than the PPN, the percentage of labeled neurons (7.2–16.1%) was similar. No FG+/ChAT+ neurons were found in the LDTd. Figure 4 shows cell plots of FG+/ChAT+, FG−/ChAT+, and FG+/ChAT− neurons in sections obtained from five different rostrocaudal levels of the mesopontine tegmentum. Together, Figures 3 and 4 show the following results: The FG+/ChAT+ neurons were intermingled with FG−/ChAT+ neurons. Although every rostrocaudal level of the PPN contained some FG+/ChAT+ neurons, most were found in the caudoventral part of PPN; in particular, the highest number was in the section 0.5–0.7 mm caudal to the 4^{th} nucleus. Also, the section containing the largest number of FG+/ChAT+ neurons was always 240 μm rostral to the one containing the largest number of ChAT+ neurons. The labeled neurons in the PPN contralateral to FG injection were distributed in similar locations relative to the ipsilateral PPN.

The existence of FG+/ChAT+ neurons in other brain areas was also examined. Though there were no FG+/ChAT+ neurons in the basal forebrain area, the caudal midline thalamus, or the hypothalamus, we found a few (less than 4 neurons per section) small (approximately 200 μm^2) FG+/ChAT+ neurons in the cuneiform nucleus, the parabrachial nucleus, and the dorsal and medial raphe nuclei.

Numbers of ChAT− mesopontine-STN projection neurons

Figures 3 and 4 also show the numbers and distributions of FG+/ChAT− neurons in the mesopontine tegmentum. FG+/ChAT− neurons were found in a wide area surrounding the superior cerebellar peduncle, including the RRF, ventral part of DMN, PPN, LDTv, and in the very dorsal most part of PnO. The total number of FG+/ChAT− neurons in these areas ipsilateral to FG-injected STN was 320–480, which was approximately 9 times that of FG+/ChAT+ neurons in PPN. The contralateral side also contained a large number of FG+/ChAT− neurons, 131–195, which is approximately 40% of the number in the ipsilateral side. Although FG+/ChAT− neurons were distributed over a wide area, they were the most prevalent in the mid-rostrocaudal region of the mesopontine tegmentum. The section containing the most FG+/ChAT-neurons was 240 μm caudal to the 4th nucleus and also 240 μm rostral to the section containing the largest number of FG+/ChAT+ neurons. In the section containing the most FG+/ChAT− neurons, a small area containing a dense gathering of FG+/ChAT− neurons was found dorsomedial to the ChAT+ neuron-rich caudolateral PPN. The area may correspond to the MEA defined by Rye et al., (1987). The boundary of this area could not be delineated from the sections immunostained for ChAT or NeuN, thus a 0.5 mm × 1.0 mm tilted box was used to approximate the area, and the percentage of FG+/ChAT− neurons over the total number of ChAT− neurons was calculated (Fig. 2C). The percentages of FG+/ChAT− neurons ranged from 57.4% to 69.6%, with a mean of 61.0±5.8 % (mean±S.D., n=4). The LDTv also contained a small number of FG+/ChAT− neurons (Fig. 3C and 4).

FG injection into the ZI

To evaluate effects of spreading of FG injection sites into the ZI on the data described above, FG was injected into the ZI. Of a total of 7 injections, 3 covered a large area of ZI without spreading to the STN and were considered successful injections (Fig. 5A). The 4 other injections covered both ZI and STN. The results of the 3 successful cases were used for comparing the locations of FG+/ChAT+ and FG+/ChAT-neurons in the mesopontine tegmentum to those observed after FG injection into the STN. The cell counts of FG+/ChAT+ neurons in the PPN for the 3 rats were 20, 23, and 28. More than half of these FG+/ChAT+ neurons were found in the caudodorsal part of the PPN. The caudoventral region of PPN, which contained FG+/ChAT+ neurons after FG injections into STN, also contained scattered FG+/ChAT+ neurons after FG injections into the ZI (Fig. 5B–D). The caudomedial part of PPN contained only one FG+/ChAT+ neuron in one rat and none in the other two cases. Unlike STN injections, ZI injections resulted in relatively large numbers of FG+/ChAT+ neurons (9, 10, and 12) in the LDTd.

FG+/ChAT− neurons were found in various areas of the mesopontine tegmentum including the RRF, the deep layers of the superior colliculus, DMN, the central gray, and in the dorsal half of PnO. Scattered FG+/ChAT− neurons were also found in the PPN. However, FG injection into the ZI did not label many neurons in the MEA (Fig. 5C and D).

BDA anterograde neurotracing

The primary aim of BDA anterograde neurotracing studies was to confirm that the area containing FG+ neurons sends axons to the STN. As expected from the study by Bevan and Bolam (1995), BDA injections involving the PPN labeled two types of fibers in the STN:

thin fibers with small en-passant varicosities and slightly thicker fibers that traverse the STN from dorsomedial to ventrolateral and give off collaterals with clumps of larger boutons (referred to as fibers with small varicosities and fibers with large boutons, hereafter) (Fig. 6C). The BDA injections in the mesopontine tegmentum also resulted in granular labeling of a small number of frontal cortical, pallidal, and STN neurons, which were possible candidates for neurons projecting both to the STN and the mesopontine tegmentum. It was unlikely that the axons in the STN belonged to those neurons containing granular labeling because the light microscopic morphology of the two types of axons differed from the known morphology of the cortical, GPe, and STN axons in the STN. The short diameters of the small en-passant varicosities and clumps of large boutons were estimated to be 0.3–0.9μm (average 0.57±0.16μm, n=100) and 0.4–1.4μm (0.98±0.22μm, mean±S.D., n=100). The measurements were made by observing them under x100 oil-immersion objective and referring the short diameters to a calibrated scale projected in the camera lucida. The fibers with small varicosities were very similar to ChAT+ fibers described in previous studies in human (Mesulam et al., 1992) and rat STN (Bevan & Bolam 1995) and also described in this study. The distribution of the clumps of large boutons in the STN was very patchy (Fig. 6C). Both types of fibers were also found in the ZI and the lateral hypothalamic area, and some of these also exited STN rostrolaterally into the internal capsule.

The distributions of the labeled fibers in the STN were consistent with the results of the retrograde labeling experiments described above. BDA injections in the area that was identified as having abundant FG+/ChAT− neurons described above resulted in the labeling of a moderate to large number of fibers with large boutons and sparse labeling of thin fibers with small varicosities (Figs. 6, 7B). In contrast, BDA injections made in areas that were identified as being sparsely populated with FG+/ChAT− neurons resulted in the labeling of only a small number of fibers with large boutons (e.g., Figs. 7A, 7C). BDA injections into the caudoventral portion of the PPN, where a large number of FG+/ChAT+ neurons were found, resulted in the labeling of a dense plexus of thin fibers with small varicosities (so dense, in fact, that they could not be reliably plotted under microscope observation) and a moderate number of fibers with large boutons in the STN. The rostral 2/3 of STN contained more fibers with large boutons than the caudal 1/3 of STN in all 8 cases. BDA injection into the area rich with FG+/ChAT− neurons also retrograde-labeled a small number of STN neurons, which is consistent with previous reports (Edley, & Graybiel, 1983;Kita & Kitai, 1987;Smith et al., 1990).

Discussion

The mesopontine tegmentum has a wide range of afferent and efferent connections between various areas of the central nervous system including the basal ganglia and is involved in the control of sensorimotor, associative, sleep wakefulness, and other limbic functions. The present study was to characterize in detail the cholinergic and non-cholinergic mesopontine projections to the STN, which plays key roles in the control of basal ganglia activity (Bevan et al., 2002; Kita et al., 2005).

Cholinergic PPN-STN projection neurons

Mesopontine cholinergic neurons send massive dorsally and ventrally coursing ascending fibers. The dorsally coursing fibers project to various thalamic nuclei, while the ventrally coursing fibers project to some of the basal ganglia nuclei and limbic structures including the ventral tegmental area, SNc, STN, ZI, lateral hypothalamus, caudate-putamen, ventral part of the globus pallidus, ventral pallidum, medial septal nucleus, vertical limb of the diagonal band area, and the central and medial nuclei of the amygdala (Graybiel, 1977; McBride & Larsen, 1980; Nomura et al., 1980; Carpenter et al., 1981; Saper & Loewy, 1982; Hammond et al., 1983; Jackson & Crossman, 1983; Spann & Grofova 1991; Woolf &

Butcher, 1986; Rye et al., 1987; Lee et al., 1988; Hallanger & Wainer, 1988; Woolf et al., 1990; Mesulam et al., 1992; Semba & Fibiger 1992; Lavoie & Parent, 1994; Bevan & Bolam 1995). A single cell labeling study revealed that cholinergic PPN neurons innervate multiple structures through extensive collaterals (Mena-Segovia et al., 2008). These cholinergic afferents are part of reticular activating systems (Steriade, 2004 & 2006), and involved in the generation of various state dependent oscillations in functionally related areas of brain (Steriade 2006; Mena-Segovia et al., 2008). The present results confirmed that the rat STN receives abundant cholinergic innervations from the mesopontine area and implied that PPN cholinergic neurons control basal ganglia oscillations in normal and pathological conditions through the STN. The cholinergic axons were thin and laden with numerous small en-passant varicosities similar to human STN (Mesulam et al., 1992). Bevan and Bolam (1995) established that these small varicosities of similar size to those in this study form synapses, which indicates that all of the cholinergic fibers that enter into the STN may form synapses with STN neurons. The present results also revealed the somatic size, number, and location of the cholinergic neurons involved in the mesopontine-STN projections. The somatic size of ChAT+ neurons in the PPN and LDTv was significantly larger than the ChAT− neurons. However, ChAT+ neurons in the cuneiform nucleus, parabrachial nucleus, and dorsal and medial raphe nuclei were small (as reported previously, see Oakman et al., 1999), with a very small number of these being FG+. There was no evidence of FG+/ChAT+ neurons in the basal forebrain area, the caudal midline thalamus, or the hypothalamus. These observations, together with the lesion results, indicate that cholinergic axons in the STN originate mainly from large ChAT+ neurons in the PPN and a few small ChAT+ neurons in other mesopontine regions.

FG injection into the STN resulted in the strong labeling of a small number of ChAT+ PPN neurons. The total number of ChAT+ neurons in PPN was estimated to be 3694 (average of 4 rats) in this study, which was ≈25% larger than the previous estimate 2942 using a stereological method (Mena-Segovia et al., 2009). The present number may be a slight overestimate due to the counting method used in this study. The total number of the ChAT+ neurons projecting to the STN was estimated to be about 360 in the homolateral side and about 80 in the contralateral side (approximately and respectively 10% and 2% of the total ChAT+ PPN neurons). It is possible that these numbers are slight over-estimates because the FG injections had small spreading into the ZI, and direct FG injections into the ZI labeled ChAT+ neurons in the PPN. After FG injections into the STN, more FG+/ChAT+ neurons were found in the caudoventral region of the PPN. The section containing the most FG+/ ChAT+ neurons was not the one containing the largest number of ChAT+ neurons. BDA injections in the same area resulted in the labeling of numerous thin fibers with small en-passant varicosities in STN. The density of labeled fibers was too high to be plotted under microscopic observation.

FG injection into the ZI resulted in the labeling of FG+/ChAT+ neurons mainly in the dorsal region of PPN and LDTd, although occasional FG+/ChAT+ neurons were observed in similar locations to those seen after FG injections into STN. The total number of FG+/ChAT + neurons observed in the PPN after FG injections into ZI was approximately half of those after STN injections. These observations imply that the cholinergic neurons participating in the STN and ZI projections are small populations of mostly separate groups. There were also very small numbers of FG+/ChAT+ neurons in the LDTv after FG injections into the STN. It has been shown that the SNc and the ventral tegmental area receive cholinergic innervations mainly from the PPN and LDTv, respectively (Cornwall et al., 1990; Semba & Fibiger, 1992; Steininger et al., 1992; Oakman et al., 1995). It is possible that the subpopulations of PPN and LDTv neurons that project to the SNc and the ventral tegmental area also project to the STN.

Non-cholinergic PPN-STN projection neurons

The non-cholinergic PPN-STN projections have also been described by a number of investigators. However, the extent and location of neurons involved in this projection have not yet been characterized. The results of the present FG retrograde and BDA anterograde experiments suggest that a relatively large number of neurons in the mesopontine tegmentum project to the STN. The number of neurons involved in these projections is estimated to be 3300 in the homolateral side and 1300 in the contralateral side. These numbers may be slightly overestimated due to the limitations of the counting method. The total numbers of non-cholinergic neurons are approximately 9 times higher than those of cholinergic neurons. FG injections into the STN labeled a large number of FG+/ChAT− neurons in a small area of DMN at approximately 0.5 mm caudal to the 4th nucleus. Based on the location and the paucity of ChAT+ neurons, this area may correspond with the MEA, which has strong reciprocal connections to the globus pallidus internal segment (GPi) and SNr (Rye et al., 1987, Lee et al., 1988). FG injection into the ZI labeled ChAT− neurons in a wide area of the mesopontine tegmentum. The labeling was dense in the RRF, central gray, and PnO, while labeling was sparse in the MEA. The areas labeled after FG injection into STN and ZI were partially overlapped. Thus, like the estimates for ChAT+ neurons, the number of the STN projecting neurons could be slightly overestimated.

The results of the BDA anterograde labeling were generally consistent with the results of the retrograde labeling experiments: BDA injections in various parts of the mesopontine tegmentum consistently labeled thicker fibers with aggregated patches of larger boutons in a wide area including the STN, ZI, and the lateral hypothalamus. The STN contains large glutamatergic terminals of unknown origin (Bevan et al., 1995). It is possible that they may belong to mesopontine afferent fibers. The present results suggested that STN receives non-cholinergic innervations from a wide area of the mesopontine tegmentum. Although it is possible that this diffuse projection pattern is due to the labeling of both STN-projecting and non-STN-projecting neurons by each BDA injection, some neurons may innervate to multiple sites, which is characteristic of the mesopontine-diencephalic projections reported in previous studies (Woolf & Butcher, 1986; Oakman et al., 1999). Of the 10 BDA injections, an injection into the MEA labeled the largest number of fibers with large boutons in the STN. Even in this case, the density was moderate enough for the boutons in the STN to be plotted under the light microscope. It is possible that each non-cholinergic neuron forms a small number of terminals in the STN. The results of the FG and BDA tracing experiments suggest that STN and ZI receive non-cholinergic inputs from partially overlapped, but largely segregated, areas of the mesopontine tegmentum.

Functional implications

The present study revealed that a small population of cholinergic neurons located mainly in the caudoventral part of the PPN form dense innervations in the STN. Also, a relatively large number of non-cholinergic neurons, many of which are in the area dorsomedial to the caudal part of PPN, project to the STN and form aggregated patches of boutons. It has been demonstrated that most of the telencephalic and diencephalic basal ganglia connections are unilateral, while the present study established that both cholinergic and non-cholinergic mesopontine-STN projections are bilateral. Both cholinergic and non-cholinergic PPN neurons receive inhibitory inputs from the GPi and SNr (Granata & Kitai, 1991; Shink et al., 1997; Grofova & Zhou, 1998), implying basal ganglia outputs provide direct inhibitory control over the activity of the mesopontine neurons. The currently available physiological studies suggest that the cholinergic projections are excitatory to STN neurons (Hammond et al., 1983; Capozzo et al., 2009) and are mediated by muscarinic receptors (Feger et al., 1979). There is no detailed physiological study on the non-cholinergic innervations. Thus, the STN, SNc, and basal ganglia output nuclei directly receive state dependent activity

information from cholinergic and non-cholinergic neurons in the mesopontine tegmentum (Mena-Segovia et al., 2008).

A significant population of PPN cholinergic neurons was shown to undergo degeneration in idiopathic PD (Hirsch et al., 1987; Jellinger, 1988; Zweig et al., 1989). Neuronal and metabolic activities of PPN-STN neurons in 6-OHDA treated rat model of PD were greatly increased (Carlson, et al., 1999; Orieux, et al., 2000; Breit et al., 2001). It is possible that the PPN neurons projecting to the STN are vulnerable to a slowly progressive form of PD. However, one study reported no loss of PPN cholinergic neurons in two animal models of PD, MPTP treated monkeys and 6-OHDA treated rats (Heise, 2005). It is not currently known whether or not the small non-cholinergic neurons were lost in PD. Low frequency (15–25 Hz) stimulation of the PPN or injection of $GABA_A$ antagonist in the PPN improves akinesia and gait dysfunction in PD patients and animal models of PD (Nandi et al., 2002; Jenkinson et al., 2004; Plaha & Gill, 2005; Stefani et al., 2007). The improvement could involve modulations of STN neuronal activity by cholinergic or non-cholinergic PPN afferent inputs (Galati et al., 2008; Capozzo et al., 2009, Galati et al., 2008). Another possibility is that stimulation of mesopontine cholinergic afferents activates a wide area of the dorsal thalamus as an ascending reticular activation system and improves motor and non-motor functions by controlling the level of activation in each functional system (Steriade, 2004). Understanding the roles that these mesopontine-STN projections play in the control of basal ganglia functions and in the development of PD requires further studies.

Acknowledgments

We thank R. Kita for editing the manuscript. This work was supported by NIH grants NS-47085 and NS-57236.

Abbreviations

Anatomical

3	oculomotor nucleus
4	trochlear nucleus
4n	trochlear nerve
CnF	cuneiform nucleus
DMN	deep mesencephalic nucleus
DR	dorsal raphe nucleus
GPi	internal segment of the globus pallidus
ic	internal capsule
IP	interpeduncular nucleus
LDT	laterodorsal tegmental nuclei
LDTd	dorsal laterodorsal tegmental nuclei
LTDv	ventral laterodorsal tegmental nuclei
ll	lateral lemniscus
MEA	midbrain extrapyramidal area
ml	medial lemniscus
Mit	microcellular tegmental nucleus

mlf	medial longitudinal fasciculus
PR	pontine raphe nucleus
scp	superior cerebellar peduncle
PnO	pontine reticular nucleus oral part
PSTh	parasubthalamic nucleus
PPN	pedunculopontine tegmental nucleus
RRF	retrorubral field
SNc	substantia nigra pars compacta
SNr	substantia nigra pars reticulata
STN	subthalamic nucleus
ZI	zona incerta

Others

ABC	avidin-biotin peroxidase complex
BDA	biotinylated dextran amine
ChAT	choline acetyltransferase
ChAT+	ChAT-immunopositive
ChAT−	ChAT-immunonegative (non-cholinergic)
FG	Fluoro-Gold
FG+	FG labeled
FG−	FG negative
NeuN	neuron-specific nuclear protein
NeuN+	NeuN-immunopositive
PBS	phosphate buffered saline
PD	Parkinson’s disease

Literature

Bevan MD, Bolam JP. Cholinergic, GABAergic, and glutamate-enriched inputs from the mesopontine tegmentum to the subthalamic nucleus in the rat. J Neurosci. 1995; 15:7105–7120. [PubMed: 7472465]

Bevan MD, Francis CM, Bolam JP. The glutamate-enriched cortical and thalamic input to neurons in the subthalamic nucleus of the rat: convergence with GABA-positive terminals. J Comp Neurol. 1995; 361:491–511. [PubMed: 8550895]

Bevan MD, Magill PJ, Terman D, Bolam JP, Wilson CJ. Move to the rhythm: oscillations in the subthalamic nucleus-external globus pallidus network. Trends Neurosci. 2002; 25:525–531. [PubMed: 12220881]

Breit S, Bouali-Benazzouz R, Benabid AL, Benazzouz A. Unilateral lesion of the nigrostriatal pathway induces an increase of neuronal activity of the pedunculopontine nucleus, which is reversed by the lesion of the subthalamic nucleus in the rat. Eur J Neurosci. 2001; 14:1833–1842. [PubMed: 11860479]

Capozzo A, Florio T, Confalone G, Minchella D, Mazzone P, Scarnati E. Low frequency stimulation of the pedunculopontine nucleus modulates electrical activity of subthalamic neurons in the rat. J Neural Transm. 2009; 116:51–56. [PubMed: 19034381]

Carlson JD, Pearlstein RD, Buchholz J, Iacono RP, Maeda G. Regional metabolic changes in the pedunculopontine nucleus of unilateral 6-hydroxydopamine Parkinson's model rats. Brain Res. 1999; 828:12–19. [PubMed: 10320720]

Carpenter MB, Carleton SC, Keller JT, Conte P. Connections of the subthalamic nucleus in the monkey. Brain Res. 1981; 224:1–29. [PubMed: 7284825]

Carpenter MB, Jayaraman A. Subthalamic nucleus of the monkey: connections and immunocytochemical features of afferents. J Hirnforsch. 1990; 31:653–668. [PubMed: 1707079]

Chang HT, Kuo H, Whittaker JA, Cooper NG. Light and electron microscopic analysis of projection neurons retrogradely labeled with Fluoro-Gold: notes on the application of antibodies to Fluoro-Gold. J Neurosci Methods. 1990; 35:31–37. [PubMed: 1703614]

Clements JR, Grant S. Glutamate-like immunoreactivity in neurons of the laterodorsal tegmental and pedunculopontine nuclei in the rat. Neurosci Lett. 1990; 120:70–73. [PubMed: 2293096]

Cornwall J, Cooper JD, Phillipson OT. Afferent and efferent connections of the laterodorsal tegmental nucleus in the rat. Brain Res Bull. 1990; 25:271–284. [PubMed: 1699638]

Edley SM, Graybiel AM. The afferent and efferent connections of the feline nucleus tegmenti pedunculopontinus, pars compacta. J Comp Neurol. 1983; 217:187–215. [PubMed: 6886052]

Feger J, Hammond C, Rouzaire-Dubois B. Pharmacological properties of acetylcholine-induced excitation of subthalamic nucleus neurones. Br J Pharmacol. 1979; 65:511–515. [PubMed: 427326]

Galati S, Scarnati E, Mazzone P, Stanzione P, Stefani A. Deep brain stimulation promotes excitation and inhibition in subthalamic nucleus in Parkinson's disease. Neuroreport. 2008; 19:661–666. [PubMed: 18382282]

Granata AR, Kitai ST. Inhibitory substantia nigra inputs to the pedunculopontine neurons. Exp Brain Res. 1991; 86:459–466. [PubMed: 1761086]

Graybiel AM. Direct and indirect preoculomotor pathways of the brainstem: an autoradiographic study of the pontine reticular formation in the cat. J Comp Neurol. 1977; 175:37–78. [PubMed: 886026]

Grofova I, Zhou M. Nigral innervation of cholinergic and glutamatergic cells in the rat mesopontine tegmentum: light and electron microscopic anterograde tracing and immunohistochemical studies. J Comp Neurol. 1998; 395:359–379. [PubMed: 9596529]

Hallanger AE, Wainer BH. Ascending projections from the pedunculopontine tegmental nucleus and the adjacent mesopontine tegmentum in the rat. J Comp Neurol. 1988; 274:483–515. [PubMed: 2464621]

Hammond C, Rouzaire-Dubois B, Feger J, Jackson A, Crossman AR. Anatomical and electrophysiological studies on the reciprocal projections between the subthalamic nucleus and nucleus tegmenti pedunculopontinus in the rat. Neuroscience. 1983; 9:41–52. [PubMed: 6308507]

Heise CE, Teo ZC, Wallace BA, Ashkan K, Benabid AL, Mitrofanis J. Cell survival patterns in the pedunculopontine tegmental nucleus of methyl-4-phenyl-1,2,3,6-tetrahydropyridine-treated monkeys and 6OHDA-lesioned rats: evidence for differences to idiopathic Parkinson disease patients? Anat Embryol (Berl). 2005; 210:287–302. [PubMed: 16237536]

Hirsch EC, Graybiel AM, Duyckaerts C, Javoy-Agid F. Neuronal loss in the pedunculopontine tegmental nucleus in Parkinson disease and in progressive supranuclear palsy. Proc Natl Acad Sci U S A. 1987; 84:5976–5980. [PubMed: 3475716]

Jackson A, Crossman AR. Subthalamic projection to nucleus tegmenti pedunculopontinus in the rat. Neurosci Lett. 1981; 22:17–22. [PubMed: 6164022]

Jackson A, Crossman AR. Nucleus tegmenti pedunculopontinus: efferent connections with special reference to the basal ganglia, studied in the rat by anterograde and retrograde transport of horseradish peroxidase. Neuroscience. 1983; 10:725–765. [PubMed: 6646427]

Jenkinson N, Nandi D, Miall RC, Stein JF, Aziz TZ. Pedunculopontine nucleus stimulation improves akinesia in a Parkinsonian monkey. Neuroreport. 2004; 15:2621–2624. [PubMed: 15570164]

Jellinger K. The pedunculopontine nucleus in Parkinson's disease, progressive supranuclear palsy and Alzheimer's disease. J Neurol Neurosurg Psychiatry. 1988; 51:540–543. [PubMed: 3379428]

Kita H, Kitai ST. Efferent projections of the subthalamic nucleus in the rat: light and electron microscopic analysis with the PHA-L method. J Comp Neurol. 1987; 260:435–452. [PubMed: 2439552]

Kita H, Tachibana Y, Nambu A, Chiken S. Balance of monosynaptic excitatory and disynaptic inhibitory responses of the globus pallidus induced after stimulation of the subthalamic nucleus in the monkey. J Neurosci. 2005; 25:8611–8619. [PubMed: 16177028]

Lavoie B, Parent A. Pedunculopontine nucleus in the squirrel monkey: cholinergic and glutamatergic projections to the substantia nigra. J Comp Neurol. 1994; 344:232–241. [PubMed: 7915727]

Lee HJ, Rye DB, Hallanger AE, Levey AI, Wainer BH. Cholinergic vs. noncholinergic efferents from the mesopontine tegmentum to the extrapyramidal motor system nuclei. J Comp Neurol. 1988; 275:469–492. [PubMed: 2461392]

Manaye KF, Zweig R, Wu D, Hersh LB, De Lacalle S, Saper CB, German DC. Quantification of cholinergic and select non-cholinergic mesopontine neuronal populations in the human brain. Neuroscience. 1999; 89:759–770. [PubMed: 10199611]

Mena-Segovia J, Bolam JP, Magill PJ. Pedunculopontine nucleus and basal ganglia: distant relatives or part of the same family? Trends Neurosci. 2004; 27:585–588. [PubMed: 15374668]

Mena-Segovia J, Micklem BR, Nair-Roberts RG, Ungless MA, Bolam JP. GABAergic neuron distribution in the pedunculopontine nucleus defines functional subterritories. J Comp Neurol. 2009; 515:397–408. [PubMed: 19459217]

Mena-Segovia J, Sims HM, Magill PJ, Bolam JP. Cholinergic brainstem neurons modulate cortical gamma activity during slow oscillations. J Physiol. 2008; 586:2947–2960. [PubMed: 18440991]

Mesulam MM, Mufson EJ, Wainer BH, Levey AI. Central cholinergic pathways in the rat: an overview based on an alternative nomenclature (Ch1-Ch6). Neuroscience. 1983; 10:1185–1201. [PubMed: 6320048]

McBride RL, Larsen KD. Projections of the feline globus pallidus. Brain Res. 1980; 189:3–14. [PubMed: 6153920]

Nandi D, Aziz TZ, Giladi N, Winter J, Stein JF. Reversal of akinesia in experimental parkinsonism by GABA antagonist microinjections in the pedunculopontine nucleus. Brain. 2002; 125:2418–2430. [PubMed: 12390969]

Nomura S, Mizuno N, Sugimoto T. Direct projections from the pedunculopontine tegmental nucleus to the subthalamic nucleus in the cat. Brain Res. 1980; 196:223–227. [PubMed: 7397521]

Oakman SA, Faris PL, Cozzari C, Hartman BK. Characterization of the extent of pontomesencephalic cholinergic neurons' projections to the thalamus: comparison with projections to midbrain dopaminergic groups. Neuroscience. 1999; 94:529–547. [PubMed: 10579214]

Oakman SA, Faris PL, Kerr PE, Cozzari C, Hartman BK. Distribution of pontomesencephalic cholinergic neurons projecting to substantia nigra differs significantly from those projecting to ventral tegmental area. J Neurosci. 1995; 15:5859–5869. [PubMed: 7666171]

Orieux G, Francois C, Feger J, Yelnik J, Vila M, Ruberg M, Agid Y, Hirsch EC. Metabolic activity of excitatory parafascicular and pedunculopontine inputs to the subthalamic nucleus in a rat model of Parkinson's disease. Neuroscience. 2000; 97:79–88. [PubMed: 10771341]

Paxinos, G.; Watson, C. The Rat Brain in Stereotaxic Coordinates. 4. Academic Press; San Diego, USA: 1998.

Plaha P, Gill SS. Bilateral deep brain stimulation of the pedunculopontine nucleus for Parkinson's disease. Neuroreport. 2005; 16:1883–1887. [PubMed: 16272872]

Reiner A, Veenman CL, Medina L, Jiao Y, Del Mar N, Honig MG. Pathway tracing using biotinylated dextran amines. J Neurosci Methods. 2000; 103:23–37. [PubMed: 11074093]

Rye DB, Saper CB, Lee HJ, Wainer BH. Pedunculopontine tegmental nucleus of the rat: cytoarchitecture, cytochemistry, and some extrapyramidal connections of the mesopontine tegmentum. J Comp Neurol. 1987; 259:483–528. [PubMed: 2885347]

Saper CB, Loewy AD. Projections of the pedunculopontine tegmental nucleus in the rat: evidence for additional extrapyramidal circuitry. Brain Res. 1982; 252:367–372. [PubMed: 7150958]

Schmued LC, Fallon JH. Fluoro-Gold: a new fluorescent retrograde axonal tracer with numerous unique properties. Brain Res. 1986; 377:147–154. [PubMed: 2425899]

Semba K, Fibiger HC. Afferent connections of the laterodorsal and the pedunculopontine tegmental nuclei in the rat: a retro- and antero-grade transport and immunohistochemical study. J Comp Neurol. 1992; 323:387–410. [PubMed: 1281170]

Shink E, Sidibe M, Smith Y. Efferent connections of the internal globus pallidus in the squirrel monkey: II. Topography and synaptic organization of pallidal efferents to the pedunculopontine nucleus. J Comp Neurol. 1997; 382:348–363. [PubMed: 9183698]

Smith Y, Hazrati LN, Parent A. Efferent projections of the subthalamic nucleus in the squirrel monkey as studied by the PHA-L anterograde tracing method. J Comp Neurol. 1990; 294:306–323. [PubMed: 2332533]

Spann BM, Grofova I. Nigropedunculopontine projection in the rat: an anterograde tracing study with phaseolus vulgaris-leucoagglutinin (PHA-L). J Comp Neurol. 1991; 311:375–388. [PubMed: 1720145]

Stefani A, Lozano AM, Peppe A, Stanzione P, Galati S, Tropepi D, Pierantozzi M, Brusa L, Scarnati E, Mazzone P. Bilateral deep brain stimulation of the pedunculopontine and subthalamic nuclei in severe Parkinson's disease. Brain. 2007; 130:1596–1607. [PubMed: 17251240]

Stefani A, Roberto C, Livia B, Mariangela P, Alberto C, Salvatore G, Fabio P, Andrea R, Cesare I, Francesco M, Antonella P. Non-motor functions in parkinsonian patients implanted in the pedunculopontine nucleus: Focus on sleep and cognitive domains. J Neurol Sci. 2009

Steininger TL, Rye DB, Wainer BH. Afferent projections to the cholinergic pedunculopontine tegmental nucleus and adjacent midbrain extrapyramidal area in the albino rat. I. Retrograde tracing studies. J Comp Neurol. 1992; 321:515–543. [PubMed: 1380518]

Steriade M. Acetylcholine systems and rhythmic activities during the waking--sleep cycle. Prog Brain Res. 2004; 145:179–196. [PubMed: 14650916]

Steriade M. Grouping of brain rhythms in corticothalamic systems. Neuroscience. 2006; 137:1087–1106. [PubMed: 16343791]

Wang HL, Morales M. Pedunculopontine and laterodorsal tegmental nuclei contain distinct populations of cholinergic, glutamatergic and GABAergic neurons in the rat. Eur J Neurosci. 2009; 29:340–358. [PubMed: 19200238]

Woolf NJ, Butcher LL. Cholinergic systems in the rat brain: III. Projections from the pontomesencephalic tegmentum to the thalamus, tectum, basal ganglia, and basal forebrain. Brain Res Bull. 1986; 16:603–637. [PubMed: 3742247]

Woolf NJ, Harrison JB, Buchwald JS. Cholinergic neurons of the feline pontomesencephalon. II. Ascending anatomical projections. Brain Res. 1990; 520:55–72. [PubMed: 2207647]

Zweig RM, Jankel WR, Hedreen JC, Mayeux R, Price DL. The pedunculopontine nucleus in Parkinson's disease. Ann Neurol. 1989; 26:41–46. [PubMed: 2549845]

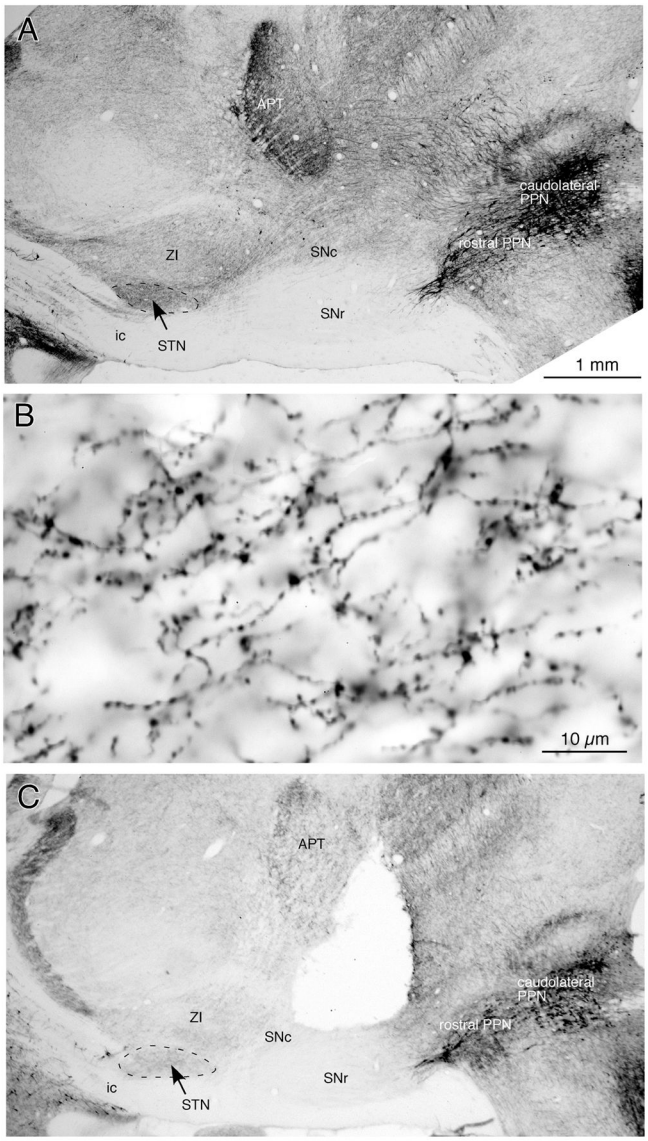

Fig. 1.

Photomicrographs of sagittal sections immunostained for ChAT. A: A low magnification view shows a large number of ChAT+ neurons in the PPN. The STN contains a dense plexus of ChAT+ fibers, and ZI contains a moderate number of ChAT+ fibers. The SNc also contains a moderate number of ChAT+ fibers, while the SNr contains very few. B: A high magnification view of ChAT+ fibers in the STN. Thin ChAT+ fibers with numerous small boutons en-passant run from the caudodorsal to rostroventral direction. C: Electrical lesions of the midbrain tegmentum extending from the deep layers of the superior colliculus to the SNc greatly reduced the ChAT+ fibers in the STN and ZI. See Abbreviations list for the abbreviations used in this and subsequent figures.

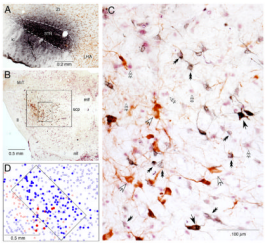

Fig. 2.

FG injection into the STN retrogradely labeled ChAT+ and ChAT− neurons in the mesopontine tegmentum. A: A photomicrograph of an FG injection site that covers most of the STN, outlined by a dashed line, with little spreading to the ZI. B and C: Low (B) and high (C) magnification photomicrographs of a mesopontine tegmentum section stained with FG (stained dark-blue), ChAT (brown), and NeuN (purple). C: The high magnification view shows the small rectangular area marked in B, in which FG+/ChAT+ (some are marked by large black arrows), FG−/ChAT+ (large white arrows), FG+/NeuN+ (small black double headed arrows), and FG−/NeuN+ (small white double headed arrows) neurons are visible. D: A drawing of the area marked by the large box in B shows the distribution of FG+/ChAT + (filled red dots), FG−/ChAT+ (open red dots), FG+/NeuN immunoreactive (filled blue dots), and FG−/NeuN+ (open blue dots) neurons. The area marked with a tilted rectangular box contains a large number of FG+/NeuN+ neurons (details in Results).

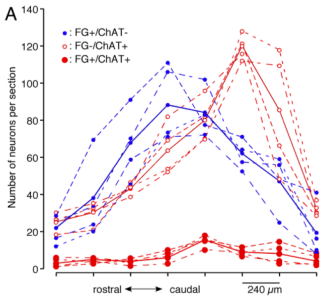

B Numbers of FG+/ and FG-/ChAT+ neurons in PPN and LDTv

	PPN			LDTv		
	Ipsi		Contra	Ipsi		Contra
	FG+	FG-	FG+	FG+	FG-	FG+
Rat 1	47	427	10	4	51	0
Rat 2	46	433	6	9	57	1
Rat 3	56	402	12	9	47	1
Rat 4	31	405	10	5	42	1

C Numbers of FG+/ChAT- neurons in RRF, DMN, PPN, PnO, and LDTv

	RRF, DMN, PPN and PnO		LDTv	
	Ipsi	Contra	Ipsi	Contra
Rat 1	320	146	6	7
Rat 2	334	131	26	14
Rat 3	480	146	27	8
Rat 4	443	195	20	16

Fig. 3.

The number of FG+/ChAT+, FG−/ChAT+, and FG+/ChAT− neurons observed in the PPN of 4 rats after FG injections into the STN. Neurons were counted from 8 sections collected from every 8th cut (i.e., rostrocaudal distance between the two sections was 240μm). A: A graphic presentation of the results obtained from the ipsilateral PPN, with the dots connected with dashed lines showing data from individual rats and those connected with solid line showing the average. B and C: The same data obtained from the PPN and LDTv are presented in tables.

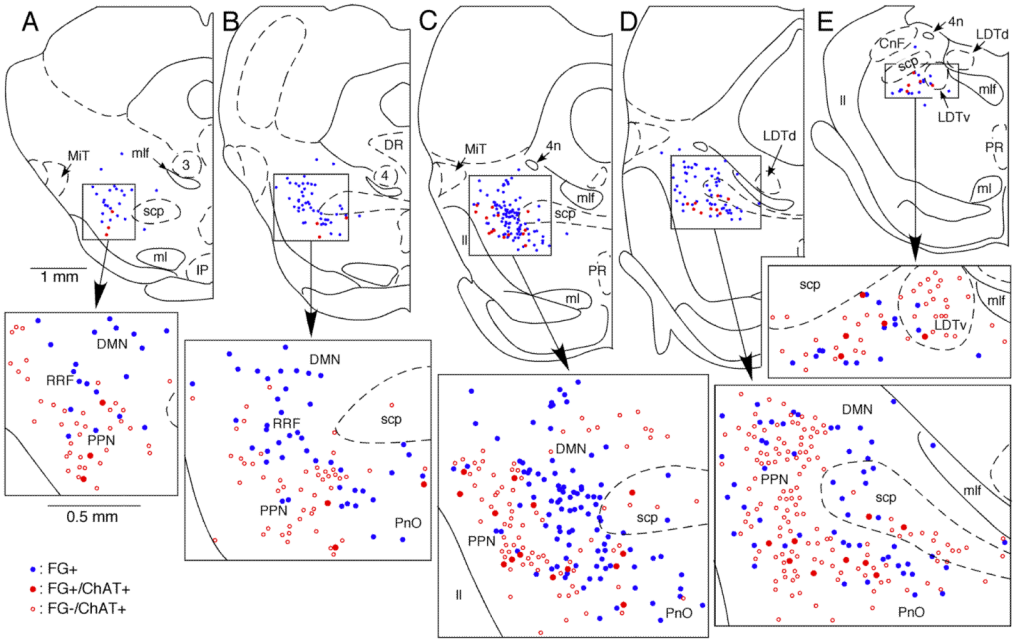

Fig. 4.

Drawings of sections showing the distributions of FG+/ChAT+, FG−/ChAT+, and FG+/ChAT− neurons in the mesopontine tegmentum after an FG injection into the STN. FG+/ChAT+ and FG+/ChAT− neurons are plotted in the low magnification drawings in the upper row. In the high magnification drawings in the lower row, FG−/ChAT+ neurons are plotted in addition to the FG+/ChAT+ and FG+/ChAT− neurons.

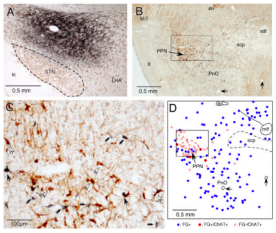

Fig. 5.

FG injection into the ZI retrogradely labeled ChAT+ and ChAT− neurons in the mesopontine tegmentum. A: A photomicrograph of an FG injection site that covers a large part of the ZI. B and C: Low (B) and high (C) magnification photomicrographs of a mesopontine tegmentum section stained with FG (stained dark-blue) and ChAT (brown). C: The high magnification view shows the small rectangular area marked in B, in which FG+/ChAT+ (some are marked by large black arrows), FG−/ChAT+ (large white arrows), and FG+/ChAT− (small black double headed arrows) neurons are visible. D: A drawing of the section shown in B shows the distribution of FG+/ChAT+ (filled red dots), FG−/ChAT+ (open red dots), and FG+/ChAT− (filled blue dots) neurons. Two small arrows point to blood vessels that were drawn in D as location references.

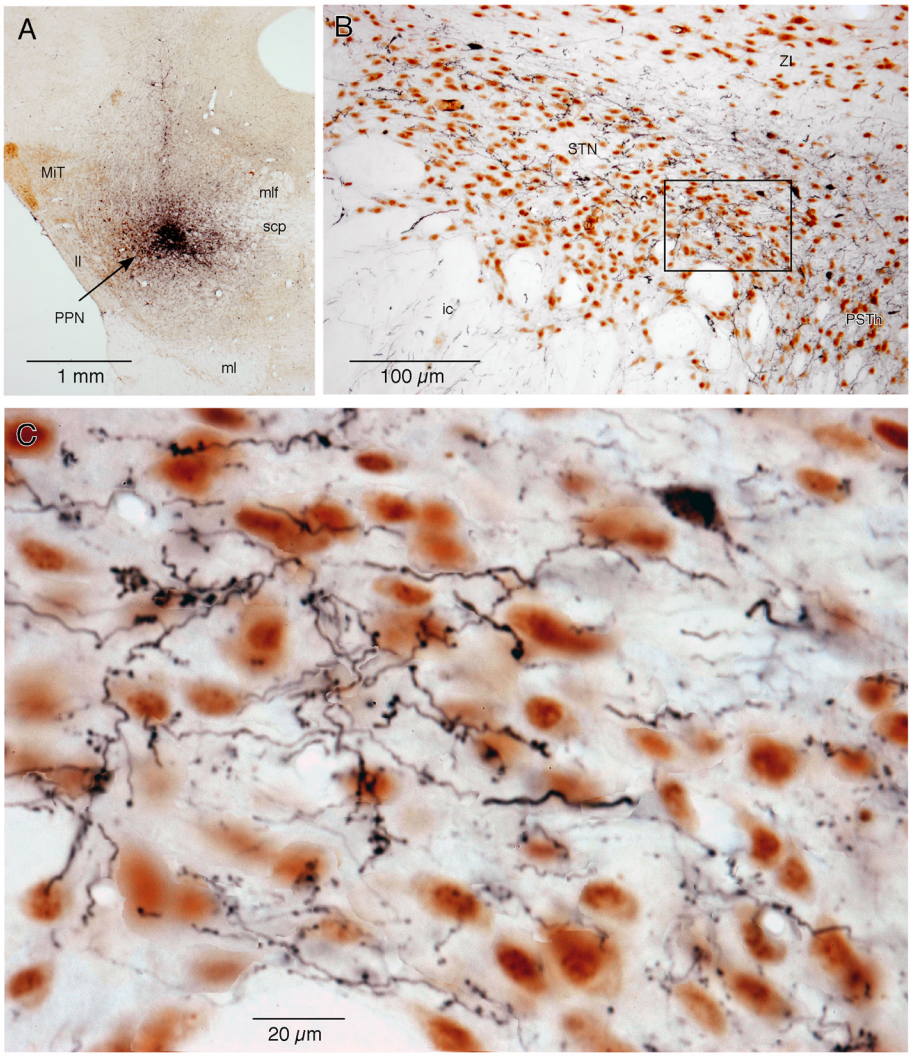

Fig. 6.

Photomicrographs show BDA-labeled fibers in the STN after BDA injection into the PPN. A: A section doubly stained for BDA and ChAT. The BDA injection site was dorsomedial to the PPN. B: A section doubly stained for BDA and NeuN. BDA-labeled fibers can be seen in the STN, ZI, ic, and PSTh. C: A high magnification view of the area marked by the box in B. Two types of fibers, thin fibers with small en passant varicosities and slightly thicker fibers with clumps of larger boutons, can be seen in the STN. The area also contains a retrograde-labeled STN neuron.

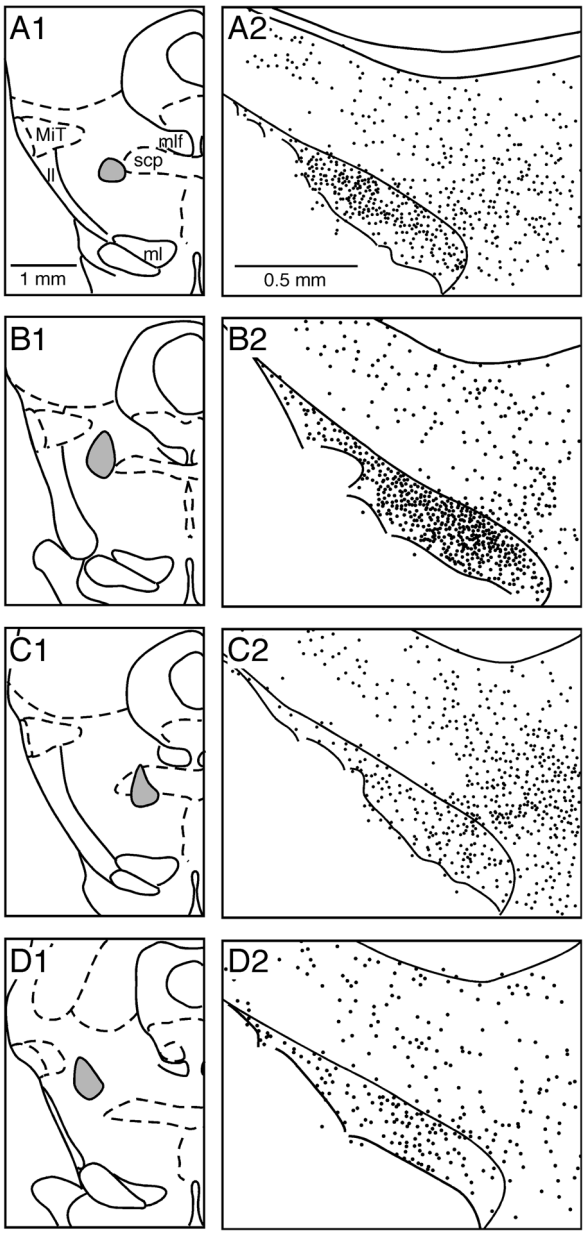

Fig. 7.

Distribution of BDA-labeled large boutons belonging to thick fibers in the STN and ZI after BDA injection into the PPN. Drawings of 4 coronal sections show the results of BDA injection in 4 different sites of PPN. Only large boutons belonging to thick fibers, approximately 5 boutons per dot, were plotted.